



Hepatic changes following a high-fat diet: effects of *Cornus mas* and gold nanoparticles phytoextracted with *Cornus mas* on oxidative stress, inflammation, and histological damage

Dalina Diana Zugravu¹, Stefan Lucian Popa², Andrei-Vasile Pop², Remus Moldovan¹, Alexandru Flaviu Tăbăran³, Luminita David⁴, Simona Valeria Clichici¹

1) Department of Physiology, Faculty of Medicine, Iuliu Hatieganu University of Medicine and Pharmacy, Cluj-Napoca, Romania

2) Second Medical Department, Iuliu Hatieganu University of Medicine and Pharmacy, Cluj-Napoca, Romania

3) Department of Anatomic Pathology, Faculty of Veterinary Medicine, University of Agricultural Sciences and Veterinary Medicine, 400372 Cluj-Napoca, Romania

4) Department of Chemistry, Faculty of Chemistry and Chemical Engineering, "Babes-Bolyai" University, Cluj-Napoca, Romania

Abstract

Background and aims. High fat diet (HFD) can lead to liver injury, through oxidative stress and inflammation. The use of natural compounds with antioxidant and anti-inflammatory properties can have a protective potential. We aimed to investigate the effects of *Cornus mas* (CM) and gold nanoparticles phytoextracted with CM (GNPsCM) on hepatic alterations induced by HFD in rats.

Methods. Female Sprague Dawley rats were randomly divided into four groups: control, HFD, HFD +CM and HFD + GNPsCM. The high fat diet was administered for 32 weeks and CM and GNPsCM were administered for 4 weeks after the HFD period. The high fat diet induced oxidative stress in liver, with lipid peroxidation and decreased antioxidant capacity, inflammation and minimal histological alterations.

Results. The administration of CM and GNPsCM reduced lipid peroxidation produced by HFD and increased antioxidant potential in liver homogenates, while increasing inflammatory markers. Histological alterations were slightly improved by the intervention of compounds, and hyaluronic acid content of the liver without statistical significance as compared to HFD group.

Conclusion. These findings support the potential of these treatments in addressing liver oxidative stress, mitigating liver damage induced by a high-fat diet. This investigation sheds light on the oxidative stress dynamics and histological alterations associated with high-fat diet-induced liver injury, contributing to our understanding of potential therapeutic interventions.

Keywords: oxidative stress, gold nanoparticles, liver disease, high-fat diet

DOI: 10.15386/mpr-2775

Manuscript received: 31.05.2024
Received in revised form: 22.06.2024
Accepted: 22.07.2024

Address for correspondence:
Andrei-Vasile Pop
Andreipopdr@gmail.com

This work is licensed under a Creative Commons Attribution-NonCommercial-NoDerivatives 4.0 International License <https://creativecommons.org/licenses/by-nc-nd/4.0/>

Background and aims

High-fat diet (HFD)-associated obesity is highly prevalent among patients with non-alcoholic fatty liver disease (NAFLD), which is increasingly recognized as a leading cause of liver disease globally, particularly in Western countries. Despite its high prevalence, only a small subset of affected individuals progress to more severe forms of the disease, such as non-alcoholic steatohepatitis (NASH), which is characterized by inflammation and varying degrees of fibrosis [1].

This progression can ultimately result in severe liver conditions such as cirrhosis and hepatocellular carcinoma, presenting substantial public health challenges [2].

The pathogenesis of NAFLD is multifactorial, involving complex interactions between genetic predispositions, metabolic factors, and environmental influences.

Despite numerous epidemiological investigations aimed at understanding this relationship, the precise mechanism underlying hepatotoxicity resulting from such dietary patterns remains elusive [3].

Table I. Risk factors for Chronic Liver Disease.

Infections	Immune system problems	Cancers and tumors	Genetic conditions	Other causes
Hepatitis A	Autoimmune hepatitis	Liver cancer	Alpha-1 antitrypsin deficiency	Alcohol abuse
Hepatitis B	Primary biliary Cholangitis	Bile duct cancer	Hemochromatosis	Drug overdose
Hepatitis C	Primary sclerosing cholangitis	Liver cell adenoma	Hyperoxaluria	Nonalcoholic fatty liver disease (NAFLD)
Hepatitis D	-	Liver cancer	Wilson's disease	Co-infection with hepatitis B, intravenous drug use
Hepatitis E	Autoimmune hepatitis	Liver cancer (although rare)	-	Alcohol abuse, contaminated water or food

Chronic liver disease (Table I) arises from a complex interplay of various factors, including infections, immune system dysregulation, cancers and tumors, genetic conditions, and numerous other causes [4].

To protect the liver health and impede the progression of liver diseases, it is essential to adopt preventive measures. These measures include minimizing exposure to hepatotoxic agents, refraining from alcohol consumption, implementing appropriate antiviral treatments when necessary, and adhering to a balanced diet [5].

Recent studies have highlighted the heightened susceptibility of hepatic diseases, including hepatocellular carcinoma, to progression in individuals experiencing overnutrition, obesity, and the consumption of lipid-rich diets [6].

Experimental studies have elucidated that animals subjected to high-fat diets often develop hepatic steatosis, a condition characterized by mononuclear inflammation and aberrant mitochondrial function. This dietary regimen also leads to insulin resistance, obesity, and disturbances in liver parameters, including elevated cholesterol and aminotransferase levels, increased triglycerides, hyperglycemia, and heightened insulin levels. Histopathological examinations following a lipid-rich diet reveal various liver tissue changes, such as steatosis, mitochondrial abnormalities, necroinflammation, pericentral fibrosis, and hepatocyte apoptosis [7,8].

Gold nanoparticles have attracted significant interest due to their exceptional optical characteristics, biocompatibility, and surface modification capacity through diverse ligand attachment [9]. Recognized for their anti-inflammatory properties, gold nanoparticles are under investigation for various medical applications. Recent investigations have positioned nanoparticles as promising delivery vehicles for both synthetic pharmaceuticals and natural compounds necessitating precise transport to target tissue cells [10].

Extensive scientific investigations have showed the multifaceted therapeutic attributes of *Cornus mas* L., the fruit of the Cornelian cherry, a member of the Cornaceae family. *Cornus mas* L. demonstrates remarkable antioxidant

and anti-inflammatory properties, primarily attributed to its rich content of iridoids, being a compelling candidate for interventions aimed at modulating lipid profiles and mitigating oxidative stress [11].

Oxidative stress is recognized as a key pathological mechanism contributing to liver injury. Various risk factors, including alcohol consumption, pharmaceutical substances, and environmental contaminants, can induce oxidative stress, leading to serious liver conditions such as alcoholic liver disease and NASH. Antioxidant therapy represents a promising approach to prevent and treat liver diseases associated with oxidative stress [12].

Glutathione (GSH), primarily found in high concentrations within the liver, serves as a crucial thiol reducing agent involved in redox regulation. GSH not only scavenges free radicals but also contributes to the balance between cellular survival, necrosis, and apoptosis [12]. The GSH/GSSG ratio reflects cellular health, and the extent of oxidative stress can be assessed by measuring malondialdehyde (MDA) levels [13].

The aim of this study was to investigate the hepatic alterations occurring after the administration of a high-fat diet compared to a control group fed a normal diet. We also aimed to assess the potential beneficial effect of the administration of solutions of *Cornus mas* or gold nanoparticles phytoreduced with *Cornus mas* on oxidative stress, inflammation markers and histological injuries produced by the high fat diet.

Methods

The study was approved by the Ethics Committee of the Iuliu Hatieganu University of Medicine and Pharmacy (No. 158/11.03.2019) and complied with Directive 86/609/EEC.

The chemicals and the methods related to the *Cornus mas* L. extract and nanoparticles synthesis were described in our previous article [14] and are just briefly described in this study.

Preparation of *Cornus mas* L. extract

Cornelian cherries were procured from the Central Market of Cluj-Napoca in August 2021, and essential

chemicals were obtained from Merck, Darmstadt, Germany. The fruits were crushed and mixed with acetone, followed by vacuum-filtration. Using a rotary evaporator, the acetone was removed to obtain a concentrated fruit extract, which was subsequently used for the phyto-reduction of gold nanoparticles. The phenolic concentration of the *Cornus mas* L. extract (CM) was quantified as grams of gallic acid equivalents per liter (GAE/L).

Synthesis and characterization of gold nanoparticles (GNPs)

The synthesis of gold nanoparticles involved a green method. Gold ions were obtained using tetrachloroauric acid and then reduced with the concentrated *Cornus mas* L. extract (GNPsCM). The colloidal solution was obtained. The characterization of GNPs was performed through UV-Vis spectroscopy, transmission electron microscopy and microelectrophoresis, as previously described [14].

Animals and diet

Sprague-Dawley female rats (n=32), 3 months old, with body weight 300 ± 10 g, purchased from Cantacuzino National Medico-Military Institute for Research and Development, Bucharest, Romania, were randomly divided into four groups (n=8 per group) for this study. The experimental diet comprised a high-fat diet (HFD), administered for 32 weeks. This diet was standardized to provide a supplemental energy increase of 45%, with a caloric value of 4.75 kcal/g, consisting of 24.3% crude protein, 21.2% crude fat, and 11.75% crude fiber. The diet was obtained from the Cantacuzino National Medico-Military Institute for Research and Development, Bucharest, Romania (Identification: ROB0001). Each rat received 20g/100g body weight per day via gavage.

Experimental design

The rats were divided into four treatment groups: (1) Control group received a standard diet for 32 weeks, then 0.5 mL/day by gavage of normal saline 0.9% from week 33 for 4 weeks (2) HFD group received high-fat diet for 32 weeks and normal saline 0.9% from week 33 for 4 weeks, (3) HFD + CM group received high-fat diet for 32 weeks and *Cornus mas* extract solution from week 33 for 4 weeks, (3) HFD + GNPsCM group received high fat diet for 32 weeks, and gold nanoparticles phyto-reduced with *Cornus mas* extract from week 33 for 4 weeks. Medication was administered between 7 a.m. and 8 a.m. at 0.5 mL/day via gastric tube gavage, with dosages of 0.158 mg/mL polyphenols for *Cornus mas* extract and 260 μ g Au/kg/day for GNPs.

Anesthesia and liver sample collection

Deep anesthesia for liver sample collection was performed using ketamine 10% (5 mg/100 g body weight) and xylazine hydrochloride 2% (100 mg/100 g body weight). Livers were collected for histopathological examination, oxidative stress, inflammation and fibrosis markers. A part of the liver was immersed in 10% formalin solution and prepared for histological analysis. The rest of the liver was

washed with cold saline and homogenized with a Polytron PT 1200E homogenizer in 50 mM TRIS+10 mM EDTA buffer (pH 7.5). The suspension was centrifuged for 10 min at 1.000 g and 4°C to separate the supernate. From each animal, supernates were stored in aliquots at -80°C until assayed. The protein levels in supernates were measured with the Bradford method. A rapid and sensitive method for the quantitation of microgram quantities of protein utilizing the principle of protein-dye binding [15].

Oxidative stress, inflammation and fibrosis investigation from liver homogenates

Oxidative stress markers, including malondialdehyde (MDA), reduced glutathione (GSH), and oxidized glutathione (GSSG), glutathione peroxidase (GSH-Px) and catalase were analyzed. MDA was assessed using the fluorometric method described by Conti et al. [16], with liver homogenate samples heated in a boiling water bath for one hour with a solution containing 10 mM 2-thiobarbituric acid in a 75 mM K₂HPO₄ solution (pH 3.0). The reaction product was extracted using n-butanol, and MDA concentration was determined spectrofluorometrically (excitation at 534 nm and emission at 548 nm), and expressed as nmol per mg of protein. GSH was measured fluorometrically using o-phthalaldehyde following Hu's method [17], with samples treated with 10% trichloroacetic acid, centrifuged, and diluted with sodium phosphate buffer. Fluorescence was recorded (excitation at 350 nm and emission at 420 nm), with GSH concentration determined using a standard curve and expressed as nmol per mg of protein. The GSH/GSSG ratio was calculated as a crucial marker of oxidative stress. For antioxidant activity, glutathione peroxidase (GPx) and catalase were also determined.

Glutathione peroxidase (GSH-Px) is a selenoprotein that catalyzes the reaction between a hydroperoxide (e.g., H₂O₂) and glutathione (GSH) as an electron donor, leading to the formation of oxidized glutathione (GSSG) and water. The determination of GSH-Px activity is performed using an indirect method based on monitoring the decrease in NADPH concentration, in the presence of which GSSG formed in the reaction is converted back to GSH by glutathione reductase (GSSG-R). The working method consists of monitoring the change in NADPH extinction at 340 or 365 nm in a reaction medium containing 2.4 U/ml glutathione reductase, 10 mM GSH, 1.5 mM NADPH, and 1.5 mM H₂O₂ in 0.1 M phosphate buffer at pH 7 for 6 minutes. The enzyme activity is defined as the amount of glutathione peroxidase that induces a net decrease of 10% of the initial GSH concentration in one minute at 37°C and pH 7. Activity is reported per 1 mg of hemoglobin for erythrocyte lysates or per 1 mg of protein for tissue homogenates [18].

Catalase is an enzyme that reduces H₂O₂ to water. It is located in both the cytosol and peroxisomes. Catalase is considered an antioxidant enzyme because it regulates

the level of H₂O₂, which, in its absence, could increase and lead to the formation of highly reactive OH radicals. The method involves monitoring the change in absorbance of a 10 mM H₂O₂ solution in 0.05 M potassium phosphate buffer (pH 7.4) at 240 nm. One unit of activity is arbitrarily defined as the amount of enzyme that induces a decrease in absorbance of 0.43 at 25°C over 3 minutes. Activity is expressed in U/mg of protein [19].

Inflammatory markers, including IL1-alpha, TLR4, TNF- α as well as hyaluronic acid for liver fibrosis assessment were assessed using ELISA technique, with absorbance readings taken at 450 nm and data analyzed using Magellan data analysis software.

Histopathological analysis

Liver tissues were fixed in 10% neutral-buffered formalin (NBF), embedded in paraffin wax, and sectioned (2 μ m) using a rotary microtome. Sections were stained with hematoxylin-eosin (H&E) and examined under an Olympus BX51 microscope. Images were captured using an Olympus SP350 digital camera and processed with Olympus cellSens software.

Data analysis

Data were analyzed using GraphPad Prism 9.3.1 (GraphPad, San Diego, USA). Statistical analysis was performed using one-way ANOVA followed by the Tukey post-test. Results were presented as means \pm standard deviation (S.D.), with significance levels indicated as * p <0.05, ** p <0.01, *** p <0.001 and **** p <0.0001 compared to the control group.

Results

1. Liver homogenate examination

1.1. Oxidative stress assessment

Malondialdehyde (MDA) levels

The results indicate that the high-fat diet significantly affects the measured parameter, with a mean difference of -0.08 (95% CI: -0.14 to -0.02, p = 0.017) when compared to the control group.

When assessing the impact of treatments, the MDA HFD+CM group showed a significant reduction in the outcome measure compared to the HFD group alone, with a mean difference of -0.17 (95% CI: -0.24 to -0.10, p = 0.0007). Similarly, the MDA HFD+GNPsCM group also demonstrated a significant reduction, with a mean difference of -0.18 (95% CI: -0.25 to -0.12, p = 0.0003). However, there was no significant difference between the MDA HFD+CM and MDA HFD+GNPsCM groups, with a mean difference of 0.01 (95% CI: -0.05 to 0.08, p = 0.87).

Comparing the treatments to the control group, the MDA HFD+CM group had a mean difference of -0.09 (95% CI: -0.13 to -0.04, p = 0.003), and the MDA HFD+GNPsCM group had a mean difference of -0.10 (95% CI: -0.16 to -0.04, p = 0.005), both showing significant reductions in the outcome measure compared to the control. These findings suggest that both CM and GNPsCM treatments significantly

improve the parameters in the high-fat diet groups, with no notable difference in their efficacy (Figure 1).

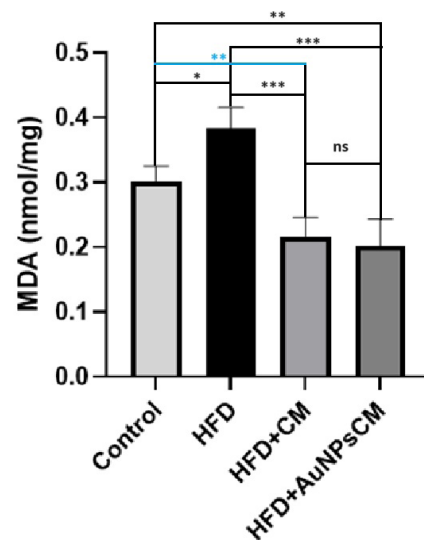


Figure 1. Malondialdehyde (MDA) Levels in Different Experimental Groups This bar graph presents the levels of malondialdehyde (MDA) in nmol/mg across four experimental groups: Control, HFD, HFD+CM, and HFD+GNPsCM. **Control:** Represents the baseline MDA levels in the control group. **HFD:** Represents the MDA levels in the group subjected to a high-fat diet. **HFD+CM:** Represents the MDA levels in the group subjected to a high-fat diet and treated with CM. **HFD+GNPsCM:** Represents the MDA levels in the group subjected to a high-fat diet and treated with Gold NPs and CM. The error bars denote the standard error of the mean (SEM). Data were analyzed using GraphPad Prism 9.3.1 (GraphPad, San Diego, USA). Statistical analysis was performed using one-way ANOVA followed by the Tukey post-test. Results were presented as means \pm standard deviation (S.D.), with significance levels indicated as ns= p >0.05, *= p <0.05, **= p <0.01, and ***= p <0.001 compared the groups between them.

GSH/GSSG (Glutathione/Glutathione Disulfide) ratio

The GSH/GSSG HFD group exhibited a significant reduction in the GSH/GSSG ratio when compared to the GSH/GSSG HFD+CM group, with a mean difference of -4.45 (95% CI: -8.77 to -0.13, adjusted p = 0.04). Similarly, a significant decrease was observed when comparing the GSH/GSSG HFD group to the GSH/GSSG HFD+GNPsCM group, showing a mean difference of -4.45 (95% CI: -8.29 to -0.61, adjusted p = 0.03). The comparison between the GSH/GSSG HFD group and the GSH/GSSG Control group also revealed a significant reduction, with a mean difference of -3.08 (95% CI: -5.94 to -0.22, adjusted p = 0.04).

No significant difference was detected between the GSH/GSSG HFD+CM group and the GSH/GSSG HFD+GNPsCM group, with a mean difference of -0.00 (95% CI: -5.55 to 5.54, adjusted p > 0.99). Additionally,

the comparison between the GSH/GSSG HFD+CM group and the GSH/GSSG Control group showed no significant difference, with a mean difference of 1.38 (95% CI: -3.73 to 6.48, adjusted $p = 0.79$). The GSH/GSSG HFD+GNPsCM group did not differ significantly from the GSH/GSSG Control group either, with a mean difference of 1.38 (95% CI: -4.13 to 6.88, adjusted $p = 0.82$).

These results indicate that the HFD group significantly reduces the GSH/GSSG ratio compared to other groups and the control, whereas no significant differences were observed among the HFD+CM, HFD+GNPsCM, and control groups (Figure 2).

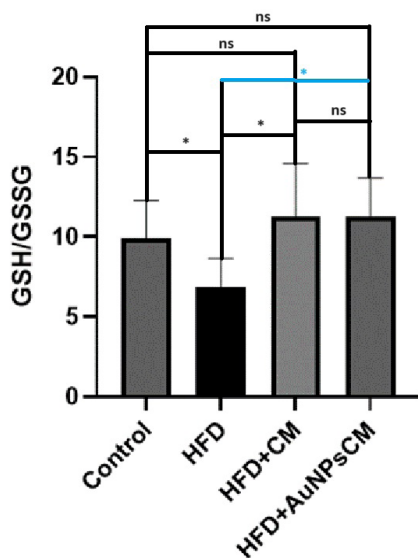


Figure 2. GSH/GSSG Ratio in Different Experimental Groups. This bar graph presents the GSH/GSSG ratio across four experimental groups: Control, HFD, HFD+CM, and HFD+GNPsCM. **Control:** Represents the baseline GSH/GSSG ratio in the control group. **HFD:** Represents the GSH/GSSG ratio in the group subjected to a high-fat diet. **HFD+CM:** Represents the GSH/GSSG ratio in the group subjected to a high-fat diet and supplemented with CM. **HFD+AuPsCM:** Represents the GSH/GSSG ratio in the group subjected to a high-fat diet and supplemented with Gold NPs and CM. The error bars denote the standard error of the mean (SEM). Data were analyzed using GraphPad Prism 9.3.1 (GraphPad, San Diego, USA). Statistical analysis was performed using one-way ANOVA followed by the Tukey post-test. Results were presented as means \pm standard deviation (S.D.), with significance levels indicated as $ns=p>0.05$, $*=p<0.05$ compared the groups between them.

Glutathione Peroxidase (GPX) levels

The GPX HFD group exhibited a significant reduction in GPX levels when compared to the GPX Control group, with a mean difference of -124.60 (95% CI: -221.50 to -27.73, adjusted $p = 0.02$). Similarly, a significant decrease was observed when comparing the GPX HFD group to the GPX HFD+GNPsCM group, showing a mean

difference of -63.88 (95% CI: -120.10 to -7.69, adjusted $p = 0.03$).

No significant difference was detected between the GPX HFD group and the GPX HFD+CM group, with a mean difference of -90.61 (95% CI: -182.30 to 1.03, adjusted $p = 0.05$). Additionally, the comparison between the GPX HFD+CM group and the GPX HFD+GNPsCM group showed no significant difference, with a mean difference of 26.74 (95% CI: -72.29 to 125.80, adjusted $p = 0.79$). The GPX HFD+CM group did not differ significantly from the GPX Control group, with a mean difference of -34.00 (95% CI: -96.44 to 28.43, adjusted $p = 0.33$). Similarly, no significant difference was found between the GPX HFD+GNPsCM group and the GPX Control group, with a mean difference of -60.74 (95% CI: -137.10 to 15.65, adjusted $p = 0.12$).

These results indicate that the GPX HFD group significantly reduces GPX levels compared to the GPX Control and GPX HFD+GNPsCM groups, whereas no significant differences were observed among the other groups (Figure 3).

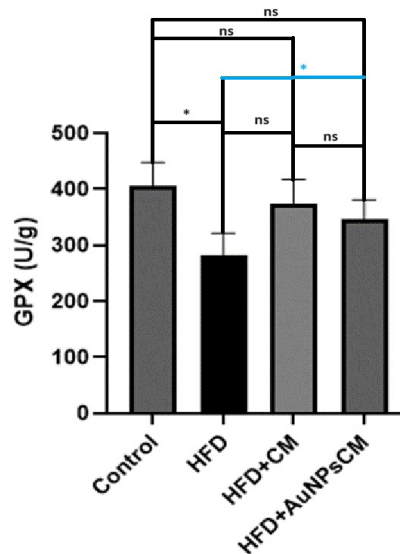


Figure 3. GPX Levels in Different Experimental Groups. This bar graph presents the GPX levels in U/g across four experimental groups: Control, HFD, HFD+CM, and HFD+GNPsCM. **Control:** Represents the baseline GPX levels in the control group. **HFD:** Represents the GPX levels in the group subjected to a high-fat diet. **HFD+CM:** Represents the GPX levels in the group subjected to a high-fat diet and supplemented with CM. **HFD+GNPsCM:** Represents the GPX levels in the group subjected to a high-fat diet and supplemented with Gold NPs and CM. The error bars denote the standard error of the mean (SEM). Data were analyzed using GraphPad Prism 9.3.1 (GraphPad, San Diego, USA). Statistical analysis was performed using one-way ANOVA followed by the Tukey post-test. Results were presented as means \pm standard deviation (S.D.), with significance levels indicated as $ns=p>0.05$, $*=p<0.05$, compared the groups between them.

1.2. Catalase levels

The GPX HFD group did not show any significant differences in catalase levels when compared to the GPX HFD+CM group, with a mean difference of -1.02 (95% CI: -30.25 to 28.20, adjusted $p = 0.99$). Similarly, no significant differences were observed when comparing the GPX HFD group to the GPX HFD+GNPsCM group, showing a mean difference of -12.39 (95% CI: -39.91 to 15.13, adjusted $p = 0.46$), and to the GPX Control group, with a mean difference of -16.25 (95% CI: -40.03 to 7.54, adjusted $p = 0.18$).

No significant differences were detected between the GPX HFD+CM group and the GPX HFD+GNPsCM group, with a mean difference of -11.37 (95% CI: -40.99 to 18.26, adjusted $p = 0.58$). Additionally, the comparison between the GPX HFD+CM group and the GPX Control group showed no significant difference, with a mean difference of -15.23 (95% CI: -41.07 to 10.62, adjusted $p = 0.27$). Similarly, no significant difference was found between the GPX HFD+GNPsCM group and the GPX Control group, with a mean difference of -3.86 (95% CI: -33.53 to 25.81, adjusted $p = 0.97$).

These results indicate that there were no significant differences in catalase levels among the HFD, HFD+CM, HFD+GNPsCM, and control groups, suggesting that none of these conditions significantly impacted the catalase levels in the experimental groups (Figure 4).

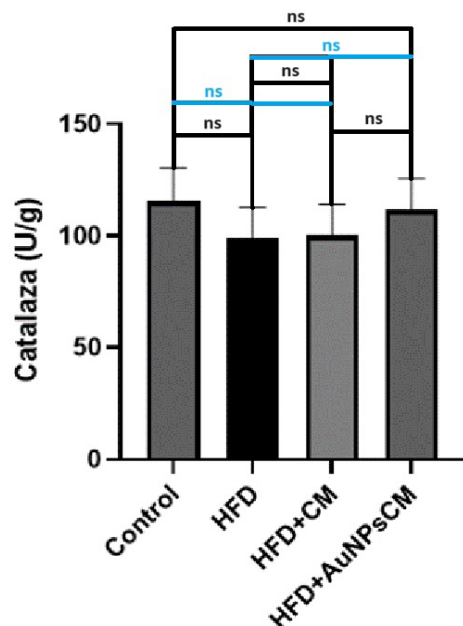


Figure 4. Catalase Levels in Different Experimental Groups

This bar graph presents the catalase (Catalaza) levels in U/g across four experimental groups: Control, HFD, HFD+CM, and HFD+GNPsCM. **Control**: Represents the baseline catalase levels in the control group. **HFD**: Represents the catalase levels in the group subjected to a high-fat diet. **HFD+CM**: Represents the catalase levels in the group subjected to a high-fat diet and supplemented with CM. **HFD+GNPsCM**: Represents the catalase

levels in the group subjected to a high-fat diet and supplemented with Gold NPs and CM. The error bars denote the standard error of the mean (SEM). Data were analyzed using GraphPad Prism 9.3.1 (GraphPad, San Diego, USA). Statistical analysis was performed using one-way ANOVA followed by the Tukey post-test. Results were presented as means \pm standard deviation (S.D.), with significance levels indicated as $ns=p>0.05$, compared the groups between them.

1.3. Inflammation assessment

TNF-alpha (Tumor Necrosis Factor-alpha) levels

The TNF alpha liver HFD group exhibited a significant reduction in TNF alpha liver levels when compared to the TNF alpha liver Control group, with a mean difference of 10.14 (95% CI: 9.65 to 10.64, adjusted $p < 0.0001$). Similarly, a significant increase was observed when comparing the TNF alpha liver HFD group to the TNF alpha liver HFD+CM group, showing a mean difference of -6.55 (95% CI: -8.15 to -4.96, adjusted $p < 0.0001$).

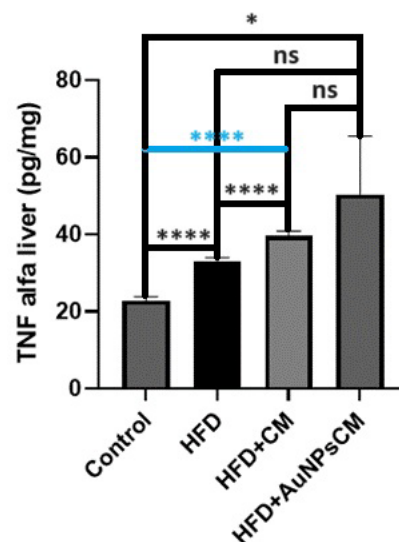


Figure 5. TNF alpha Liver Levels in Different Experimental Groups

This bar graph presents the TNF alpha liver levels in pg/mg across four experimental groups: Control, HFD, HFD+CM, and HFD+GNPsCM. **Control**: Represents the baseline TNF alpha liver levels in the control group. **HFD**: Represents the TNF alpha liver levels in the group subjected to a high-fat diet. **HFD+CM**: Represents the TNF alpha liver levels in the group subjected to a high-fat diet and supplemented with CM. **HFD+GNPsCM**: Represents the TNF alpha liver levels in the group subjected to a high-fat diet and supplemented with Gold NPs and CM. The error bars denote the standard error of the mean (SEM). Data were analyzed using GraphPad Prism 9.3.1 (GraphPad, San Diego, USA). Statistical analysis was performed using one-way ANOVA followed by the Tukey post-test. Results were presented as means \pm standard deviation (S.D.), with significance levels indicated as $ns=p>0.05$, $*=p<0.05$, $**=p<0.01$, and $***=p<0.001$, $****=p<0.0001$ compared the groups between them.

No significant difference was detected between the TNF alpha liver HFD group and the TNF alpha liver HFD+GNPsCM group, with a mean difference of -17.39 (95% CI: -36.95 to 2.16, adjusted $p = 0.0783$). Additionally, the comparison between the TNF alpha liver HFD+CM group and the TNF alpha liver HFD+GNPsCM group showed no significant difference, with a mean difference of -10.84 (95% CI: -30.30 to 8.62, adjusted $p = 0.3095$). The TNF alpha liver HFD+CM group differed significantly from the TNF alpha liver Control group, with a mean difference of 16.69 (95% CI: 15.29 to 18.10, adjusted $p < 0.0001$). Similarly, a significant increase was found between the TNF alpha liver HFD+GNPsCM group and the TNF alpha liver Control group, with a mean difference of 27.54 (95% CI: 7.71 to 47.36, adjusted $p = 0.0118$).

These results indicate that the TNF alpha liver HFD group significantly increases TNF alpha liver levels compared to the TNF alpha liver Control and TNF alpha liver HFD+CM groups, whereas no significant differences were observed among the other groups (Figure 5).

IL-1 alpha (Interleukin-1 alpha) levels

The IL1 alpha HFD group exhibited a significant increase in IL1 alpha levels when compared to the HFD+GNPsCM group, with a mean difference of 1.17 (95% CI: 0.28 to 2.06, adjusted $p = 0.02$). Similarly, a significant increase was observed when comparing the IL1 alpha HFD+CM group to the HFD+GNPsCM group, showing a mean difference of 2.72 (95% CI: 0.55 to 4.90, adjusted $p = 0.02$).

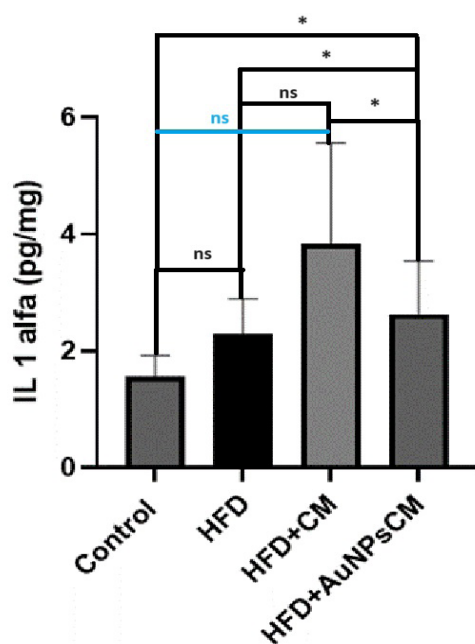


Figure 6. IL1 alfa Levels in Different Experimental Groups
This bar graph presents the IL1 alpha levels in pg/mg across four experimental groups: Control, HFD, HFD+CM, and HFD+GNPsCM. **Control:** Represents the baseline IL1 alpha

levels in the control group. **HFD:** Represents the IL1 alpha levels in the group subjected to a high-fat diet. **HFD+CM:** Represents the IL1 alpha levels in the group subjected to a high-fat diet and supplemented with CM. **HFD+GNPsCM:** Represents the IL1 alpha levels in the group subjected to a high-fat diet and supplemented with Gold NPs and CM. The error bars denote the standard error of the mean (SEM). Data were analyzed using GraphPad Prism 9.3.1 (GraphPad, San Diego, USA). Statistical analysis was performed using one-way ANOVA followed by the Tukey post-test. Results were presented as means \pm standard deviation (S.D.), with significance levels indicated as ns= $p > 0.05$, *= $p < 0.05$, compared the groups between them.

No significant difference was detected between the IL1 alpha HFD group and the IL1 alpha HFD+CM group, with a mean difference of -1.55 (95% CI: -3.69 to 0.58, adjusted $p = 0.15$), and the IL1 alpha Control group, with a mean difference of 0.73 (95% CI: -0.50 to 1.96, adjusted $p = 0.27$). Additionally, the comparison between the IL1 alpha HFD+CM group and the IL1 alpha Control group showed no significant difference, with a mean difference of 2.28 (95% CI: -0.10 to 4.66, adjusted $p = 0.06$). However, a significant decrease was found between the HFD+GNPsCM group and the IL1 alpha Control group, with a mean difference of -0.44 (95% CI: -0.87 to -0.02, adjusted $p = 0.04$).

These results indicate that the IL1 alpha HFD group significantly increases IL1 alpha levels compared to the HFD+GNPsCM group, and the IL1 alpha HFD+CM group significantly increases IL1 alpha levels compared to the HFD+GNPsCM group, whereas no significant differences were observed among the other groups (Figure 6).

Toll-Like Receptor 4 (TLR4) levels

The TLR4 liver HFD group exhibited a significant increase in TLR4 liver levels when compared to the TLR4 liver HFD+CM group, with a mean difference of -0.12 (95% CI: -0.16 to -0.08, adjusted $p = 0.0003$). Similarly, a significant increase was observed when comparing the TLR4 liver HFD group to the TLR4 liver HFD+GNPsCM group, showing a mean difference of -0.20 (95% CI: -0.27 to -0.14, adjusted $p = 0.0001$), and to the TLR4 liver Control group, with a mean difference of 0.07 (95% CI: 0.04 to 0.10, adjusted $p = 0.0007$).

A significant difference was also detected between the TLR4 liver HFD+CM group and the TLR4 liver HFD+GNPsCM group, with a mean difference of -0.08 (95% CI: -0.14 to -0.02, adjusted $p = 0.0134$). Additionally, the comparison between the TLR4 liver HFD+CM group and the TLR4 liver Control group showed a significant difference, with a mean difference of 0.19 (95% CI: 0.12 to 0.25, adjusted $p = 0.0003$). Similarly, a significant increase was found between the TLR4 liver HFD+GNPsCM group and the TLR4 liver Control group, with a mean difference

of 0.27 (95% CI: 0.19 to 0.35, adjusted $p < 0.0001$).

These results indicate that the TLR4 liver HFD group significantly increases TLR4 liver levels compared to the TLR4 liver HFD+CM group, TLR4 liver HFD+GNPsCM group, and TLR4 liver Control group, whereas significant differences were also observed among the other groups (Figure 7).

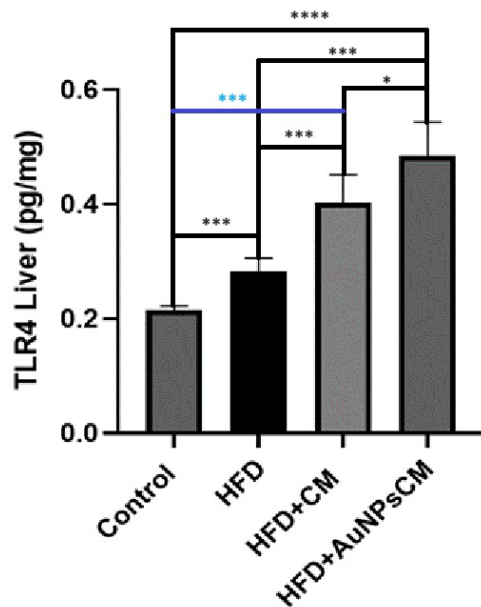


Figure 7. TLR4 Liver levels in different experimental groups This bar graph presents the TLR4 liver levels in pg/mg across four experimental groups: Control, HFD, HFD+CM, and HFD+GNPsCM. **Control:** Represents the baseline TLR4 liver levels in the control group. **HFD:** Represents the TLR4 liver levels in the group subjected to a high-fat diet. **HFD+CM:** Represents the TLR4 liver levels in the group subjected to a high-fat diet and supplemented with CM. **HFD+GNPsCM:** Represents the TLR4 liver levels in the group subjected to a high-fat diet and supplemented with Gold NPs and CM. The error bars denote the standard error of the mean (SEM). Data were analyzed using GraphPad Prism 9.3.1 (GraphPad, San Diego, USA). Statistical analysis was performed using one-way ANOVA followed by the Tukey post-test. Results were presented as means \pm standard deviation (S.D.), with significance levels indicated as ns= $p > 0.05$, *= $p < 0.05$, **= $p < 0.01$, ***= $p < 0.001$, ****= $p < 0.0001$ compared the groups between them.

1.4. Fibrosis assessment Hyaluronic acid levels

The Hyaluronic Acid HFD group exhibited a significant increase in levels when compared to the Hyaluronic Acid Control group, with a mean difference of 0.35 (95% CI: 0.07 to 0.62, adjusted $p = 0.02$). Similarly, a significant increase was observed when comparing the Hyaluronic Acid HFD+CM group to the Hyaluronic Acid Control group, showing a mean difference of 0.35 (95% CI: 0.22 to 0.48, adjusted $p = 0.0003$), and to the Hyaluronic

Acid HFD+GNPsCM group, with a mean difference of 0.33 (95% CI: 0.19 to 0.48, adjusted $p = 0.0009$).

No significant difference was detected between the Hyaluronic Acid HFD group and the Hyaluronic Acid HFD+CM group, with a mean difference of -0.00 (95% CI: -0.30 to 0.30, adjusted $p > 0.99$), and the Hyaluronic Acid HFD+GNPsCM group, with a mean difference of 0.01 (95% CI: -0.29 to 0.31, adjusted $p = 0.99$). Additionally, the comparison between the Hyaluronic Acid HFD+CM group and the Hyaluronic Acid HFD+GNPsCM group showed no significant difference, with a mean difference of 0.02 (95% CI: -0.17 to 0.20, adjusted $p = 0.99$).

These results indicate that the Hyaluronic Acid HFD group significantly increases Hyaluronic Acid levels compared to the Hyaluronic Acid Control group, whereas significant differences were also observed between the Hyaluronic Acid HFD+CM group and the Hyaluronic Acid Control group, and the Hyaluronic Acid HFD+GNPsCM group and the Hyaluronic Acid Control group (Figure 8).

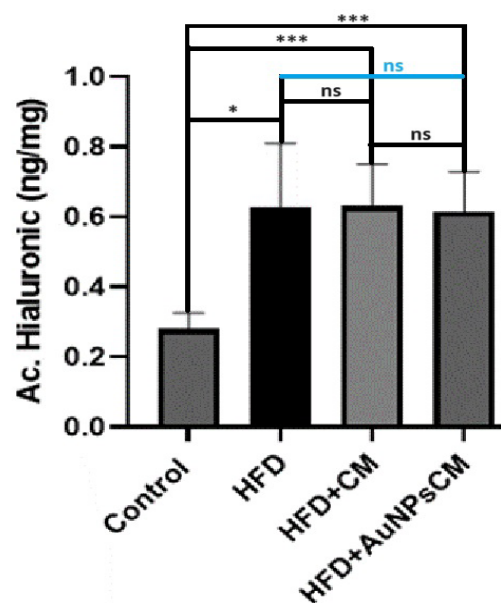


Figure 8. Hyaluronic acid levels in different experimental groups This bar graph presents the Hyaluronic Acid levels in ng/mg across four experimental groups: Control, HFD, HFD+CM, and HFD+GNPsCM. **Control:** Represents the baseline Hyaluronic Acid levels in the control group. **HFD:** Represents the Hyaluronic Acid levels in the group subjected to a high-fat diet. **HFD+CM:** Represents the Hyaluronic Acid levels in the group subjected to a high-fat diet and supplemented with CM. **HFD+GNPsCM:** Represents the Hyaluronic Acid levels in the group subjected to a high-fat diet and supplemented with Gold NPs and CM. The error bars denote the standard error of the mean (SEM). Data were analyzed using GraphPad Prism 9.3.1 (GraphPad, San Diego, USA). Statistical analysis was performed using one-way ANOVA followed by the Tukey post-test. Results were presented as means \pm standard deviation (S.D.), with significance levels indicated as ns= $p > 0.05$, *= $p < 0.05$, **= $p < 0.01$, ***= $p < 0.001$, compared the groups between them.

2. Histological examination

Histological examination of hepatic tissues from the control group (Figure 9A) showed no significant findings. In the HFD group (Figure 9B), minimal diffuse hepatocyte glycogenosis was observed, with no significant findings within the portal spaces. The HFD + GNPsCM group (Figure 9C) exhibited minimal zonal (mainly mid-zonal and centrolobular) glycogenosis, again with no significant findings within the portal spaces. Similarly, the HFD + CM group (Figure 9D) displayed minimal zonal (mainly mid-zonal) glycogenosis, with no significant findings within the portal spaces (Figure 9).

(Figure 9C) exhibited minimal zonal (mainly mid-zonal and centrolobular) glycogenosis, again with no significant findings within the portal spaces. Similarly, the HFD + CM group (Figure 9D) displayed minimal zonal (mainly mid-zonal) glycogenosis, with no significant findings within the portal spaces (Figure 9).

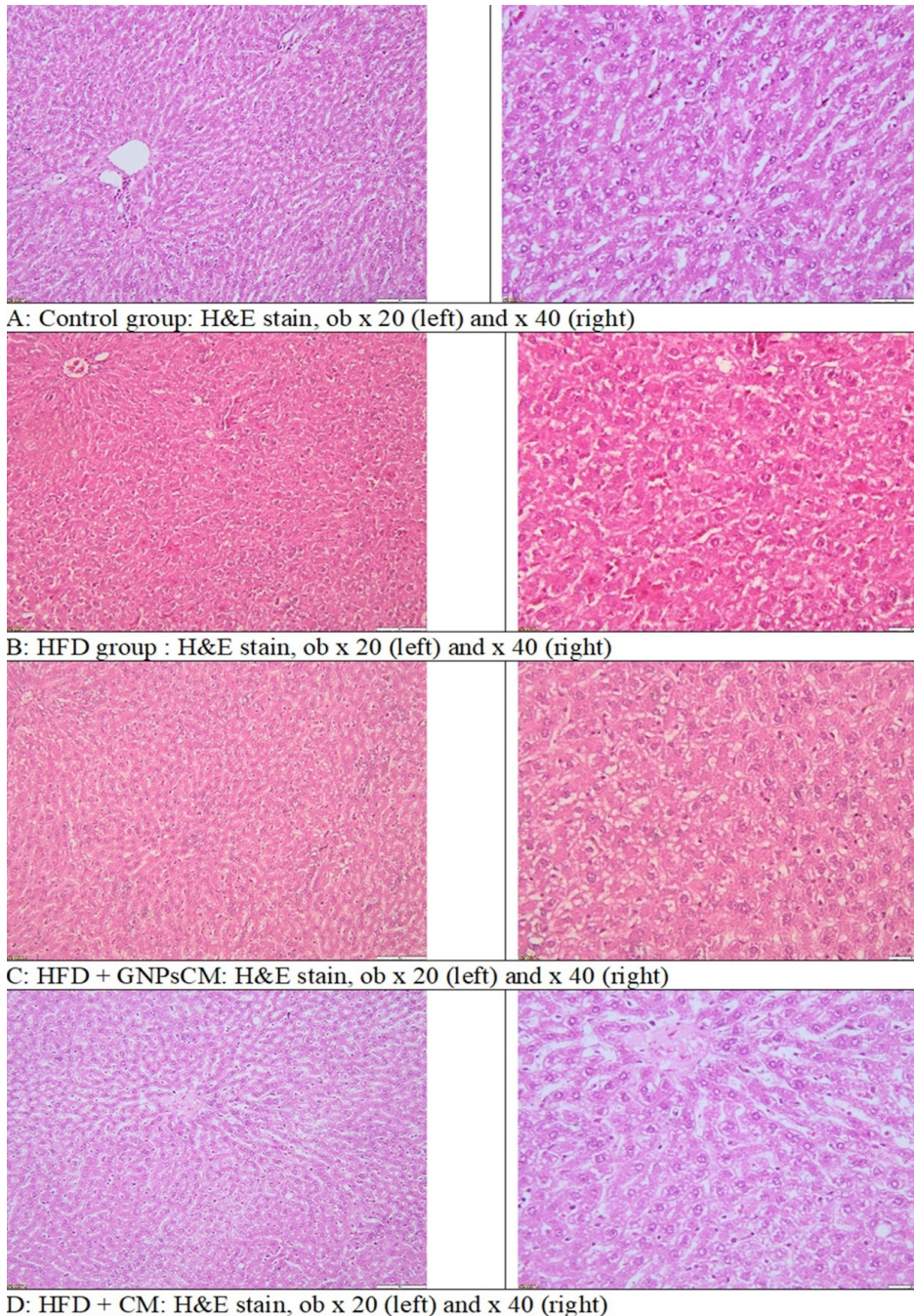


Figure 9. Hematoxylin-eosin staining of harvested hepatic tissues of rats after 9 months on HFD, with the last month including oral gavage treatment (0.9% saline solution for Control and HFD groups; Cornus mas L. extract for HFD + CM group; gold nanoparticles phytoreduced with bioactive compounds from Cornus mas L. extract for HFD + GNPsCM group).

Discussion

In this study, our objective was to comprehensively investigate the hepatic alterations induced by a high-lipid diet compared to a control group receiving a standard diet. Additionally, we aimed to evaluate whether the administration of *Cornus mas* (CM) solution and gold nanoparticles functionalized with *Cornus mas* (GNPsCM) solution could yield any hepatic improvements in the rats to which they were administered. Despite the relatively short duration of CM and GNPsCM administration in our experiment, the findings of this study underscore the profound impact of a high-fat diet on liver health, particularly highlighting the induction of hepatic steatosis, oxidative stress, and inflammation.

The significant elevation of malondialdehyde (MDA) levels in the high-fat diet (HFD) group confirms the presence of lipid peroxidation, a hallmark of oxidative stress. This is further supported by the reduced GSH/GSSG ratio, indicating compromised antioxidant defense. The administration of *Cornus mas* and gold nanoparticles (GNPs) phytoextracted with *Cornus mas* markedly improved these oxidative stress markers. The reduction in MDA levels and the restoration of the GSH/GSSG ratio in the HFD+CM and HFD+GNPsCM groups suggest that these treatments effectively enhance the antioxidant capacity of liver tissues, mitigating oxidative damage.

The observed decrease in glutathione peroxidase (GPX) levels in the HFD group corroborates the oxidative stress findings. GPX is crucial in detoxifying peroxides, and its reduction points to an overwhelmed antioxidant system. Notably, GNPsCM supplementation significantly improved GPX levels, indicating its potential to support the antioxidant defense. On the other hand, catalase levels did not show significant differences among the groups, suggesting that catalase might not be as sensitive to dietary interventions as GPX or that the oxidative stress was primarily affecting pathways beyond hydrogen peroxide detoxification.

Inflammatory markers such as TNF- α and IL-1 α were significantly elevated in the HFD group, highlighting the inflammatory response associated with high-fat diet-induced liver injury. The reduction of these markers in the HFD+CM and HFD+GNPsCM groups underscores the anti-inflammatory potential of these treatments. This anti-inflammatory effect is crucial, as chronic inflammation is a driver of fibrosis and further liver damage.

The significant increase in TLR4 levels in the HFD group is indicative of enhanced toll-like receptor signaling, which is known to play a role in inflammation and innate immunity. The marked reduction in TLR4 levels in the HFD+CM and HFD+GNPsCM groups suggests that these treatments can modulate immune responses, reducing inflammation and potentially preventing progression to more severe liver diseases.

Hyaluronic acid levels, a marker of fibrosis, were significantly elevated in the HFD group, indicating early signs of fibrotic changes. The significant reductions in hyaluronic acid levels in the HFD+CM and HFD+GNPsCM groups suggest a protective effect against fibrosis. This is particularly promising, as fibrosis is a critical step towards cirrhosis and liver failure.

Oxidative stress, characterized by an imbalance between free radical generation and antioxidant defense, emerges as a central pathological mechanism underlying liver injury [20,21]. Malondialdehyde (MDA) serves as a reliable biomarker for assessing oxidative stress levels, with elevated MDA levels indicative of increased lipid peroxidation and oxidative damage. Consistent with existing literature, our study demonstrates a decrease in MDA levels following the administration of CM and GNPsCM solutions compared to the HFD group [22,23].

In addition to MDA, our investigation focused on other oxidative stress markers, including TNF- α , IL-1 α , TLR4, GSH/GSSG ratio, GPx, catalase, and hyaluronic acid. While both CM and GNPsCM solutions exhibited a reduction in oxidative stress markers, slight disparities were observed between the two formulations. Notably, parameters such as TNF- α , IL-1 α , TLR4, GSH/GSSG ratio, and GPx showed promising outcomes post-administration of CM and GNPsCM solutions. These findings underscore the potential of both formulations in mitigating oxidative stress and liver injury.

Histological examination supported the biochemical data, showing hepatic steatosis and minimal glycogenosis in the HFD group. The improvements observed in the histological architecture of the HFD+CM and HFD+GNPsCM groups reinforce the potential therapeutic benefits of these treatments.

Our findings regarding hepatic steatosis in the high-fat diet (HFD) group are consistent with existing literature, as referenced [24], corroborating the detrimental effects of excessive dietary lipid intake on liver health [25]. However, our observations contradict those of a previous study by Romestaig et al. [26], which suggested that a high-fat diet might not induce non-alcoholic steatohepatitis (NASH) or liver steatosis due to enhanced energy dissipation in hepatic mitochondria. Our results highlight the presence of hepatic steatosis even in the context of potentially mitigating factors, underscoring the complexity of dietary-induced liver pathologies.

Furthermore, the severity of NASH/NAFLD resulting from a lipid-rich diet appears to be influenced by various factors, as mentioned [7], including diet composition, duration, and animal characteristics. For instance, the study by Nishikawa et al. [27] demonstrated elevated hepatic lipid accumulation in middle-aged C57BL/6 mice compared to their younger counterparts, emphasizing the role of age in liver lipid metabolism and disease progression. Additionally, variations in liver lipid

accumulation between different mouse strains further underscore the multifactorial nature of diet-induced liver pathologies.

In contrast, the study by Lieber et al. [28] elucidated the effects of a high-fat liquid diet on liver health in Sprague Dawley rats. Their findings indicated not only the induction of mild steatosis but also the presence of mononuclear inflammation, abnormal mitochondrial morphology, and elevated levels of inflammatory markers and oxidative stress indicators. This highlights the complex interplay between lipid intake, inflammation, and oxidative stress in the development of liver pathology.

Oxidative stress emerges as a central mechanism underlying liver injury progression, as outlined in the literature. The initiation of intracellular oxidative stress by oxidized low-density lipoprotein triggers a cascade of cellular responses, including enhanced synthesis of the p53 protein and subsequent activation of the tumor suppressor p53. These cellular responses likely contribute to necrotic and apoptotic outcomes, further exacerbating liver damage [29].

In line with this, the study by Hui Chen et al. [10] explored the potential anti-inflammatory properties of gold nanoparticles in mitigating weight gain and improving metabolic parameters in mice subjected to a high-fat diet. Their findings suggest a shift in adipose macrophages from the pro-inflammatory M1 phenotype to the anti-inflammatory M2 phenotype, highlighting the therapeutic potential of nanoparticle-based interventions in ameliorating diet-induced metabolic dysfunction.

Moreover, recent research has underscored the hepatoprotective effects of anthocyanins derived from *Cornus mas* fruit extract in animal experimental models, suggesting a potential therapeutic role in the management of non-alcoholic fatty liver disease (NAFLD). Additionally, the antioxidant properties of *Cornus mas*, attributed to its antioxidant constituents, have been shown to mitigate liver damage induced by oxidative stress [30,31]. These findings underscore the potential of natural compounds in mitigating liver injury and highlight the importance of exploring complementary therapeutic approaches for liver disorders.

The hepatoprotective effects demonstrated by *Cornus mas* (CM) and gold nanoparticles functionalized with *Cornus mas* (GNPsCM) solutions highlight the potential of natural compounds and nanoparticle-based interventions in mitigating liver injury. This underscores the importance of further research to optimize therapeutic strategies and translate these findings into clinical applications for the benefit of patients with liver diseases.

In summary, our study provides comprehensive insights into the impact of a high-lipid diet on hepatic health and the potential therapeutic effects of CM and GNPsCM solutions. By advancing our understanding of the mechanisms underlying diet-induced liver pathologies

and exploring therapeutic interventions, we contribute to the ongoing efforts to improve the management of liver disorders; by elucidating the mechanisms underlying hepatic changes in response to high-lipid diets, we enhance our knowledge of the intricate interplay between diet composition, oxidative stress, and liver pathology. Further investigations are warranted to refine therapeutic approaches and address the complex challenges posed by liver diseases in clinical settings.

Study limitations and strengths

This study's comprehensive analysis of liver homogenate revealed significant findings in oxidative stress, inflammation, and fibrosis due to a high-fat diet, with detailed assessments of MDA levels, GSH/GSSG ratio, GPX, catalase, TNF-alpha, IL1-alpha, TLR4, and hyaluronic acid. Strengths included robust statistical methods, a thorough comparison of CM and GNPsCM treatments, and histological correlation, highlighting their potential therapeutic benefits. However, limitations such as the short treatment duration, small sample size, single animal model, and lack of mechanistic insights and long-term effect evaluations suggest the need for further research to confirm and expand these findings, ensuring their applicability across diverse models and over extended periods.

Conclusion

In conclusion, our study offers valuable insights into the oxidative stress dynamics and histological changes associated with the administration of a high-fat diet in an experimental rat model. We have observed hepatic alterations indicative of liver injury, reinforcing the detrimental impact of excessive dietary lipid intake. Moreover, our findings shed light on the potential benefits of natural compounds and gold nanoparticles phytoextracted with natural compounds, particularly in mitigating oxidative stress, suggesting promising avenues for future research into nanoparticle-based interventions for liver injury.

References

1. Lian CY, Zhai ZZ, Li ZF, Wang L. High fat diet-triggered non-alcoholic fatty liver disease: A review of proposed mechanisms. *Chem Biol Interact.* 2020;330:109199.
2. Koh YC, Lin YC, Lee PS, Lu TJ, Lin KY, Pan MH. A multi-targeting strategy to ameliorate high-fat-diet- and fructose-induced (western diet-induced) non-alcoholic fatty liver disease (NAFLD) with supplementation of a mixture of legume ethanol extracts. *Food Funct.* 2020;11:7545–7560.
3. Wang X, Tanaka N, Hu X, Kimura T, Lu Y, Jia F, et al. A high-cholesterol diet promotes steatohepatitis and liver tumorigenesis in HCV core gene transgenic mice. *Arch Toxicol.* 2019;93:1713–1725.

4. WebMD. Liver disease: types of liver problems & their causes Available from: <https://www.webmd.com/hepatitis/liver-and-hepatic-diseases>
5. Kimura T, Tanaka N, Fujimori N, Sugiura A, Yamazaki T, Joshita S, et al. Mild drinking habit is a risk factor for hepatocarcinogenesis in non-alcoholic fatty liver disease with advanced fibrosis. *World J Gastroenterol*. 2018;24:1440-1450.
6. Kimura T, Kobayashi A, Tanaka N, Sano K, Komatsu M, Fujimori N, et al. Clinicopathological characteristics of non-B non-C hepatocellular carcinoma without past hepatitis B virus infection. *Hepatol Res*. 2017;47:405-418.
7. Takahashi Y, Fukusato T. Animal models of liver diseases. animal models for the study of human disease. Second Edition. 2017, p. 313-339.
8. Ioannou GN, Morrow OB, Connole ML, Lee SP. Association between dietary nutrient composition and the incidence of cirrhosis or liver cancer in the United States population. *Hepatology*. 2009;50:175-184.
9. Taghizadeh S, Alimardani V, Roudbali PL, Ghasemi Y, Kaviani E. Gold nanoparticles application in liver cancer. *Photodiagnosis Photodyn Ther*. 2019;25:389-400.
10. Chen H, Ng JPM, Tan Y, McGrath K, Bishop DP, Oliver B, et al. Gold nanoparticles improve metabolic profile of mice fed a high-fat diet. *J Nanobiotechnology*. 2018;16:11.
11. Majdan M, Bobrowska-Korczak B. Active Compounds in Fruits and Inflammation in the Body. *Nutrients* 2022;14:2496.
12. Vairetti M, Di Pasqua LG, Cagna M, Richelmi P, Ferrigno A, Berardo C. Changes in Glutathione Content in Liver Diseases: An Update. *Antioxidants (Basel)*. 2021;10:364.
13. Owen JB, Butterfiel DA. Measurement of oxidized/reduced glutathione ratio. *Methods Mol Biol*. 2010;648:269-277.
14. Moldovan R, Mitrea DR, Florea A, Chiş IC, Suciş Ş, David L, et al. Effects of Gold Nanoparticles Functionalized with Bioactive Compounds from Cornus mas Fruit on Aorta Ultrastructural and Biochemical Changes in Rats on a Hyperlipid Diet-A Preliminary Study. *Antioxidants (Basel)*. 2022;11:1343.
15. Bradford MM. A rapid and sensitive method for the quantitation of microgram quantities of protein utilizing the principle of protein-dye binding. *Anal Biochem*. 1976;72:248-254.
16. Conti M, Morand PC, Levillain P, Lemonnier A. Improved fluorometric determination of malonaldehyde. *Clin Chem*. 1991;37:1273-1275.
17. Hu ML. Measurement of protein thiol groups and glutathione in plasma. *Methods Enzymol*. 1994;233:380-385.
18. Flohé L, Günzler WA. Assays of glutathione peroxidase. *Methods Enzymol*. 1984;105:114-121.
19. Pippenger CE, Browne RW, Armstrong D. Regulatory antioxidant enzymes. *Methods Mol Biol*. 1998;108:299-313.
20. Canakci CF, Cicek Y, Yildirim A, Sezer U, Canakci V. Increased levels of 8-hydroxydeoxyguanosine and malondialdehyde and its relationship with antioxidant enzymes in saliva of periodontitis patients. *Eur J Dent*. 2009;3:100-106.
21. Li S, Tan HY, Wang N, Zhang ZJ, Lao L, Wong CW, et al. The Role of Oxidative Stress and Antioxidants in Liver Diseases. *Int J Mol Sci*. 2015;16:26087-26124.
22. Cordiano R, Di Gioacchino M, Mangifesta R, Panzera C, Gangemi S, Minciullo PL. Malondialdehyde as a Potential Oxidative Stress Marker for Allergy-Oriented Diseases: An Update. *Molecules*. 2023;28:5979.
23. Khoubnasabjafari M, Ansarin K, Jouyban A. Reliability of malondialdehyde as a biomarker of oxidative stress in psychological disorders. *Bioimpacts*. 2015;5:123-127.
24. Sasidharan SR, Joseph JA, Anandakumar S, Venkatesan V, Madhavan CN, Agarwal A. Ameliorative potential of Tamarindus indica on high fat diet induced nonalcoholic fatty liver disease in rats. *ScientificWorldJournal*. 2014;2014:507197.
25. Zhang X, Xu GB, Zhou D, Pan YX. High-fat diet modifies expression of hepatic cellular senescence gene p16(INK4a) through chromatin modifications in adult male rats. *Genes Nutr*. 2018;13:6.
26. Romestaing C, Piquet MA, Letexier D, Rey B, Mourier A, Servais S, et al. Mitochondrial adaptations to steatohepatitis induced by a methionine- and choline-deficient diet. *Am J Physiol Endocrinol Metab*. 2008;294:E110-E119.
27. Nishikawa S, Sugimoto J, Okada M, Sakairi T, Takagi S. Gene expression in livers of BALB/C and C57BL/6J mice fed a high-fat diet. *Toxicol Pathol*. 2011;40:71-82.
28. Lieber CS, Leo MA, Mak KM, Xu Y, Cao Q, Ren C, et al. Model of nonalcoholic steatohepatitis. *Am J Clin Nutr*. 2004;79:502-509.
29. Mazière C, Meignotte A, Dantin F, Conte MA, Mazière JC. Oxidized LDL induces an oxidative stress and activates the tumor suppressor p53 in MRC5 human fibroblasts. *Biochem Biophys Res Commun*. 2000;276:718-723.
30. Sangsefidi ZS, Hosseinzadeh M, Ranjbar AM, Akhondi-Meybodi M, Fallahzadeh H, Mozaffari-Khosravi H. The effect of total anthocyanin-base standardized (Cornus mas L.) fruit extract on liver function, tumor necrosis factor α , malondealdehyde, and adiponectin in patients with non-alcoholic fatty liver: a study protocol for a double-blind randomized clinical trial. *Nutr J*. 2019;18:39.
31. Alavian SM, Banihabib N, Es Haghi M, Panahi F. Protective Effect of Cornus mas Fruits Extract on Serum Biomarkers in CCl4-Induced Hepatotoxicity in Male Rats. *Hepat Mon*. 2014;14:e10330.